Peer-reviewed version available at *Energies* **2018**, *11*, 1398; doi:10.3390/en11061398

On the heat transfer enhancement of plate fin heat exchanger

Yuan Xue[1], Zhihua Ge[1], Xiaoze Du[2,*], Lijun Yang[1]

[1] Key Laboratory of Condition Monitoring and Control for Power Plant Equipment (North China Electric Power University), Ministry of Education, Beijing 102206, China

[2] School of Energy and Power Engineering, Lanzhou University of Technology, Lanzhou 730050, China

* Correspondence: duxz@ncepu.edu.cn; Tel.: +86(10)61773923; Fax. +86(10)61773877

Abstract: The plate fin heat exchanger is the compact heat exchanger applied in many industries because of its high thermal performance. To enhance the heat transfer of plate fin heat exchanger in further, three new kinds of wavy plate fins, namely perforated wavy fin, staggered wavy fin and discontinuous wavy fin are proposed and investigated by CFD simulations. The effects of key design parameters, including that of waviness aspect ratios, perforation diameters, stagger ratios and breaking distance are investigated, respectively, with the Reynolds number changes from 500 to 4500. It is found that due to the swirl flow and efficient mixing of fluid, the perforation, serration and breaking techniques are beneficial for the enhancement of heat transfer compared to the traditional wavy fin. At the same time, serration is beneficial to reduce the friction factor, and the breaking technique can reduce heat transfer area as well as enhance heat transfer performance. Through the performance evaluation criteria, the staggered wavy fin has an advantage over the small waviness aspect ratio compared to the perforated wavy fin. The maximum performance evaluation criteria (*PEC*), as high as 1.24, can be obtained for the perforated wavy fin at the largest waviness aspect ratio.

Keywords: staggered wavy fin; perforated wavy fin; discontinuous wavy fin; heat transfer enhancement

1. Introduction

As a compact heat exchanger, plate fin heat exchanger is applied in many industries and occupies a unique role due to its flexible arrangement, simple shape and good thermal effectiveness. Based on different applications, various kinds of fins are used in plate fin heat exchangers, such as plain, offset-strip, louvered, wavy and pin [1-5]. Kays and London conducted an experimental analysis of about 40 kinds of fins and offered the corresponding correlation curves of heat transfer and resistance [6]. Khoshvaght-Aliabadi investigated seven common configurations of channels used in plate fin heat exchangers experimentally. The results showed that vortex-generator channel can be applied as a high quality interrupted surface and wavy channel displayed an optimal performance in low Reynolds numbers [7]. Juan Du carried out experimental and numerical investigation of the heat transfer and pressure drop characteristics of an offset plate fin heat exchangers for cooling of lubricant oil [8]. Numerical simulations and experimental investigation of air flow and heat transfer over wavy fin were presented by Dong. The results show that the waviness amplitude has the distinct effect on the heat transfer and pressure drop of wavy fin [9].

More recently, there are still numerous researches on the development of new types of fin for heat transfer enhancement [10-12], including that of offset strip fins compact heat exchanger [13], fins with grooves or vortex generators [14, 15]. El Hassan Ridouane found that the grooves on the fin surface can enhance local heat transfer significantly [16]. Numerical simulation also found that the multi-row windward punched delta winglet on the plain fin have well enhancement performance [17]. Both experiments and numerical simulation had been conducted to investigate the air-side flow and heat transfer of the wavy fin with or without delta winglet pairs punched on the surface. The results showed that the wavy fin with delta winglet pairs can significantly enhance air-side heat transfer and pressure drop [18]. Thermal characteristics of the plan and curved vortex generators with and without punching holes in the fin surface were investigated, indicating that vortex generators with punched holes present a higher heat transfer enhancement and lower

pressure drop than that without holes [19]. In order to resolve the weakness of the louver fin heat exchanger, Chan Hyeok Jeong developed the plate fin with both ceases and holes, which were helping to improve heat transfer and could be used under hostile environments [20]. The effects of round and elongated holes were also compared [21]. It was found that the elongated holes behaved better performance but with larger pressure drops.

Among the numerous studies on the different kinds of fins, wavy and offset strip fins are the most popular ones because of their high thermal performances. Besides, punching holes on the fin surface can enhance heat transfer significantly. However, there are few studies regarding the effects of the staggered arrangement on wavy fins until now. In the present study, three kinds of wavy plate fin configurations with staggered and discontinuous arrangements are considered by numerical investigations. The benefits on heat transfer and pressure drop of the plate fin heat exchanger are analyzed accordingly.

2. Physical and Mathematic Model

2.1. Physical Model

The heat transfer performance and flow resistance of four kinds of wavy plate fins are evaluated using computational numerical analysis. Fig. 1 shows the shape and geometric details of the objective wavy fins. The traditional wavy fin was taken as comparison, three enhanced configurations shown in Fig. 1(b) to (d), including that of the perforated wavy fin, staggered wavy fin and discontinuous wavy fin, were also investigated to verify their heat transfer performances.

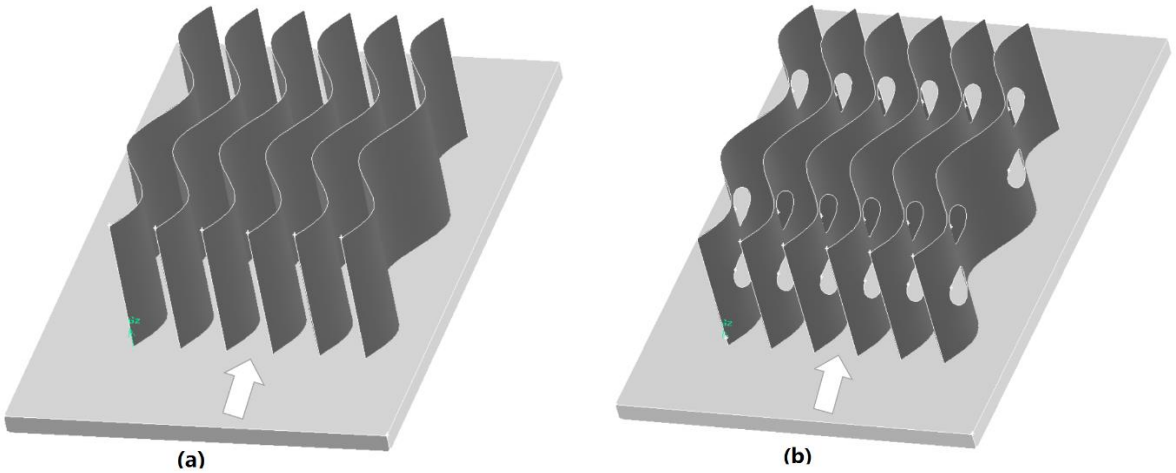

Preprints (www.preprints.org) | NOT PEER-REVIEWED | Posted: 24 April 2018 doi:10.20944/preprints201804.0304.v1

Peer-reviewed version available at Energies 2018, 11, 1398; doi:10.3390/en11061398

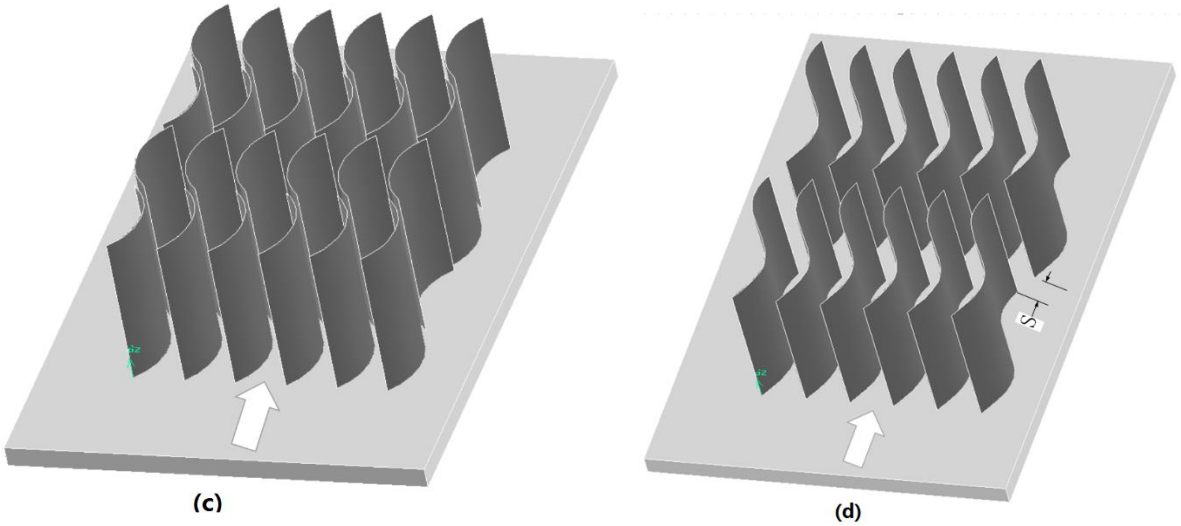

Figure 1. The shape of (a) traditional wavy fin; (b) perforated wavy fin; (c) staggered wavy fin type; (d) discontinuous wavy fin.

2.2. Governing Equations

The continuity, momentum and energy equations are listed as follows, which govern the three dimensional, steady-state flow of air flowing in the proposed wavy fin passage.

$$\frac{\partial(\rho u_i)}{\partial x_i} = 0 \tag{1}$$

$$\frac{\partial(\rho u_i u_j)}{\partial x_i} = -\frac{\partial p}{\partial x_i} + \frac{\partial}{\partial x_j}\left(\tau_{ij} - \rho\overline{u_i' u_j'}\right) \tag{2}$$

$$\frac{\partial}{\partial x_i}\left(\rho u_i C_p T\right) = \frac{\partial}{\partial x_i}\left(\lambda \frac{\partial T}{\partial x_i}\right) \tag{3}$$

in which,

$$\tau_{ij} = \mu\left(\frac{\partial u_i}{\partial x_j} + \frac{\partial u_j}{\partial x_i} - \frac{2}{3}\delta_{ij}\frac{\partial u_k}{\partial x_k}\right) \tag{4}$$

$$-\rho\overline{u_i' u_j'} = \mu_t\left(\frac{\partial u_i}{\partial x_j} + \frac{\partial u_j}{\partial x_i} - \frac{2}{3}\delta_{ij}\frac{\partial u_k}{\partial x_k}\right) - \frac{2}{3}\delta_{ij}\rho k \tag{5}$$

$$k = \frac{\overline{u_i' u_j'}}{2} \tag{6}$$

The standard $k-\varepsilon$ model, low Re $k-\varepsilon$ model, RNG $k-\varepsilon$ model and $k-\omega$ SST model are used as turbulent models for verification of calculation, finally the RNG $k-\varepsilon$ is selected because of the minimum error between the results and reference experimental data (For details, see section 3.1). The enhanced wall function was adopted to deal with the near wall region. For the RNG $k-\varepsilon$ model, the transport equations of turbulence kinetic energy, k, and dissipation rate, ε ,are followed by,

Preprints (www.preprints.org) | NOT PEER-REVIEWED | Posted: 24 April 2018 doi:10.20944/preprints201804.0304.v1

Peer-reviewed version available at Energies 2018, 11, 1398; doi:10.3390/en11061398

$$\frac{\partial}{\partial x_i}(\rho k u_i) = \frac{\partial}{\partial x_j}\left[\left(\mu + \frac{\mu_t}{\sigma_k}\right)\frac{\partial k}{\partial x_j}\right] + G_k - \rho\varepsilon \tag{7}$$

$$\frac{\partial}{\partial x_i}(\rho \varepsilon u_i) = \frac{\partial}{\partial x_j}\left[\left(\mu + \frac{\mu_t}{\sigma_\varepsilon}\right)\frac{\partial \varepsilon}{\partial x_j}\right] + C_{1\varepsilon}\frac{\varepsilon}{k}G_k - C_{2\varepsilon}\rho\frac{\varepsilon^2}{k} \tag{8}$$

and with the model constants as $C_{1\varepsilon} = 1.42 - \frac{\tilde{\eta}(1-\tilde{\eta}/\tilde{\eta}_0)}{1+\beta\tilde{\eta}^3}$, $\tilde{\eta} = Sk/\varepsilon$, $S = \left(2S_{i,j}S_{i,j}\right)^{1/2}$, $S_{i,j} = \frac{1}{2}\left(\frac{\partial u_i}{\partial x_j} + \frac{\partial u_j}{\partial x_i}\right)$, $\tilde{\eta} = 4.38$, $\beta = 0.015$, $C_{2\varepsilon} = 1.68$, $\sigma_k = 0.7179$, $\sigma_\varepsilon = 0.7179$. μ_t and G_k denote turbulent viscosity and the generation of turbulence kinetic energy because of the mean velocity gradients.

Figure 2 shows the computational domains and the boundary conditions for staggered wavy fins, where the regions enclosed by the dashed lines are designated as computational domains of the staggered wavy fins. The boundary conditions consist an inlet, an outlet, the periodic left and right, and the boundary condition of plate part is constant wall temperature that is 334 K.

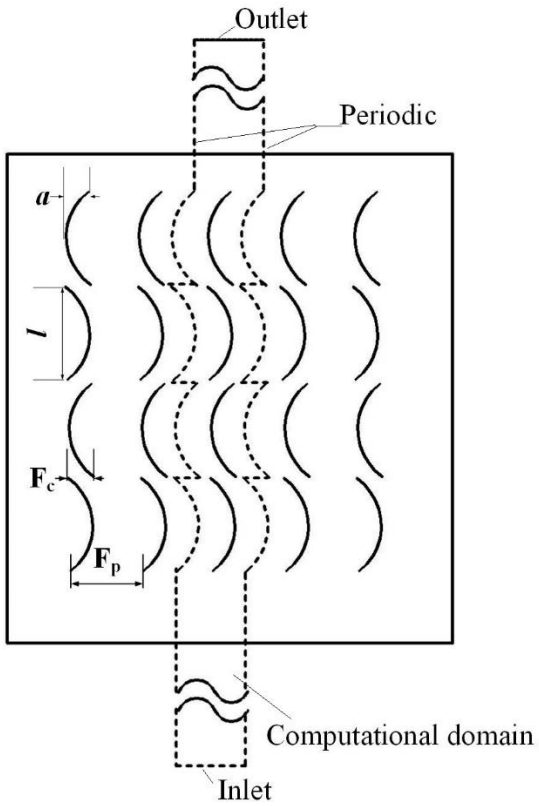

Fig 2. Computational domains and boundary details for the staggered wavy fin.

The length of the upstream zone is taken 30mm and the length of the downstream is extended to 100mm to ensure the uniformity of air inlet velocity and avoid the flow recirculation at the outlet. Computational domain inlet is defined as the velocity inlet boundary condition with the velocity ranging from 5m/s to 25m/s and the constant air inlet temperature

Preprints (www.preprints.org) | NOT PEER-REVIEWED | Posted: 24 April 2018 doi:10.20944/preprints201804.0304.v1

Peer-reviewed version available at Energies 2018, 11, 1398; doi:10.3390/en11061398

is 398 K.

2.3. Parameter Definitions

For the heat transfer performance, the air-side surface heat transfer coefficient, *h*, of the wavy fin is calculated as follows,

$$h = \frac{Q}{A \bullet \Delta T} \tag{9}$$

$$\Delta T = \frac{(T_{in} - T_w) - (T_{out} - T_w)}{\ln\left[(T_{in} - T_w)/(T_{out} - T_w)\right]} \tag{10}$$

$$Q = mC_p (T_{out} - T_{in}) \tag{11}$$

where m, C_p, T_{out}, T_{in} are the mass flow rate of air flow, specific heat, inlet and outlet bulk temperatures of air, respectively. T_w is the bottom wall temperature which is a constant, 334 K. A is the total heat transfer area of the plate and effective wavy fins, $A = A_p + \eta_f A_f$,of which, A_p is the plate surface, A_f is all fin surface that contact with air. $\eta_f = \frac{T_{f,ave} - T_{air,ave}}{T_w - T_{air,ave}}$ is the fin efficiency with $T_{air,ave} = \frac{1}{2}(T_{in} + T_{out})$.

The Reynolds number is defined as

$$\mathrm{Re} = \frac{GD_h}{\mu} \tag{12}$$

where G is the mass velocity, D_h is the hydraulic diameter for the plate staggered wavy fin channel given by Refs.[22].

$$D_h = \frac{4A_c L}{(A_p + A_f)} \tag{13}$$

where A_c is the minimum free flow area, L is the flow length.

For the proposed wavy fin studied in current study, D_h is given as

$$D_h = \frac{2(F_p - \delta)F_h L}{\left(F_p L + F_h L_z - \pi R^2\right)} \tag{14}$$

The specific geometrical feature of the wavy fin is described by the wave amplitude (a) and wavelength (*l*). The waviness aspect ratio is defined as

$$\gamma = 2a/l \tag{15}$$

For the staggered wavy fin, the stagger ratio is described as

Preprints (www.preprints.org) | NOT PEER-REVIEWED | Posted: 24 April 2018 doi:10.20944/preprints201804.0304.v1

Peer-reviewed version available at Energies 2018, 11, 1398; doi:10.3390/en11061398

$$\beta = F_c / F_p \tag{16}$$

The mean Nusselt number is described as

$$Nu = \frac{hD_h}{\lambda} \tag{17}$$

The Colburn factor and Fanning friction factor are defined as

$$j = \frac{Nu}{\mathrm{Re}\,\mathrm{Pr}^{1/3}} \tag{18}$$

$$f = \frac{\rho D_h \Delta P}{2LG^2} \tag{19}$$

where ΔP is the pressure drop between the inlet and outlet of the air channel.

For the comparison of the overall flow and heat transfer performance of the proposed wavy fins, the heat exchanger performance evaluation criteria is defined as

$$PEC = \frac{Nu / Nu_{basic,wavy}}{(f / f_{basic,wavy})^{1/3}} \tag{20}$$

2.4. Grid Independence Tests and Verification of CFD Model

The mathematical model of the turbulent flow though the wavy fin is solved using the commercial software FLUENT. The momentum and energy equations are solved by the second-order upwind scheme. The pressure-velocity coupling flow analysis is conducted using a SIMPLE algorithm.

The computational meshes are generated by software GAMBIT 2.4.6. For the region of computational domains, the structured mesh is used. For the periodic boundary, the meshes are matched by linking the periodic surfaces.

Grid independence tests are carried out before further numerical work. Three different grid numbers are adopted to examine the influence of the grid number, which include about 1,159,000, 1,600,000, and 1,930,000 cells. Fig. 3 shows the change in the *j* factor in accordance with change of grid number. As shown in Fig.3, the change of *j* factor is less when the grid number increased from 1.159 to 1.93 million. In order to study the influence of the structural parameters on the performance of proposed wavy fins, therefore, in this study, the calculation was conducted using the corresponding mesh division method of 1.60 million grid numbers.

Preprints (www.preprints.org) | NOT PEER-REVIEWED | Posted: 24 April 2018 doi:10.20944/preprints201804.0304.v1

Peer-reviewed version available at Energies 2018, 11, 1398; doi:10.3390/en11061398

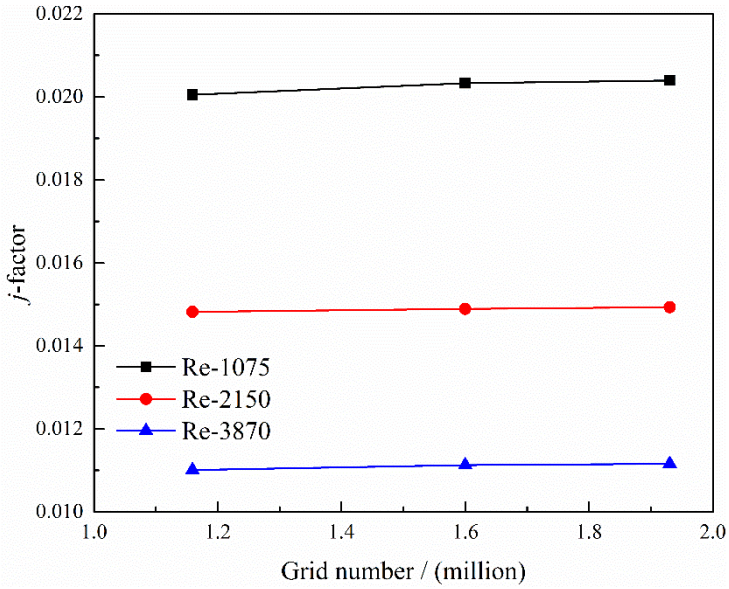

Figure 3. Change in the j-factor in accordance with the change of grids number.

Fig. 4 shows comparison between the values of the (a) j and (b) f factors using different turbulent models (standard $k-\varepsilon$ model, low Re $k-\varepsilon$ model, RNG $k-\varepsilon$ model and SST model) at Re from 1000 to 4000 for the traditional wavy fin. The values of the j and f factors obtained using the correlations presented by Dong junqi [23] with the same geometric parameters. The RNG $k-\varepsilon$ is selected because of the minimum error between the results and reference experimental data.

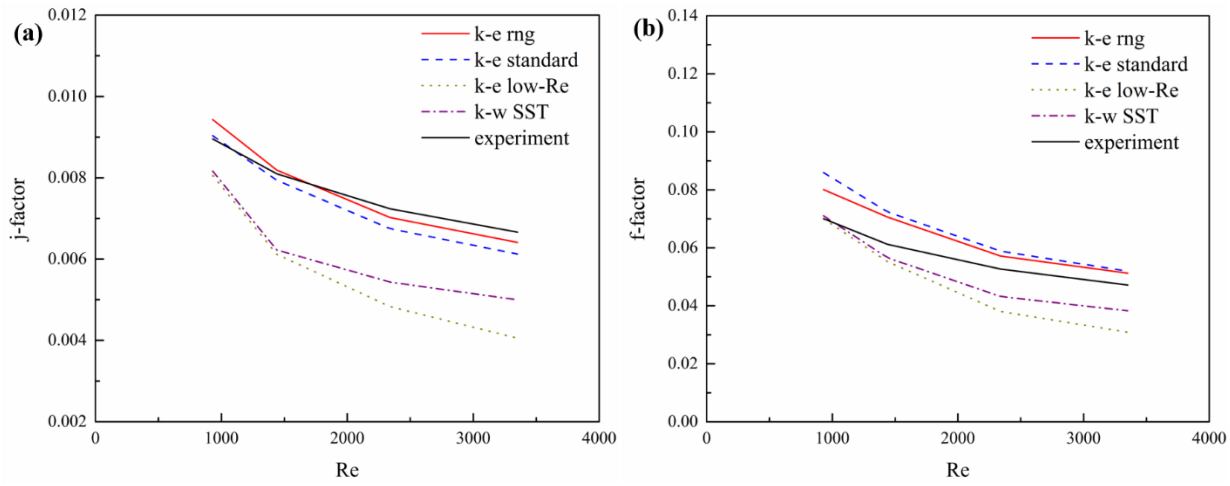

Figure 4. Comparison between the values of the (a) j-factor and (b) f-factor using different turbulent flow models.

3. Results with Analysis

3.1. Influence of Different Perforated Radius

The relation of the Nusselt number ratio ($Nu/Nu_{basic,wavy}$), friction factor ratio ($f/f_{basic,wavy}$) and the *PEC* to

Preprints (www.preprints.org) | NOT PEER-REVIEWED | Posted: 24 April 2018 doi:10.20944/preprints201804.0304.v1

Peer-reviewed version available at Energies 2018, 11, 1398; doi:10.3390/en11061398

the Reynolds number for the different perforated radius are presented in Fig. 5. Fig.6 shows the change in the streamline and fin surface temperature distribution of the perforated wavy fin with different radius. The radii of the punched holes are 0.5mm, 1mm, and 1.5mm, respectively. It can be found that at the same operating condition, the perforated wavy fin with the larger punched hole has higher values of Nusselt number and friction factor. The streamline in Fig.6 (a) shows that the enlarged hole can strengthen the flow turbulence, leading to a rapid mixing between the core and the fluid near the fin surface. From Fig. 6 (b) it can be seen that for wavy fin with larger punched holes the surface temperature of most regions is higher than those with smaller holes and it means that these fins had a better heat transfer. A surface having a high *PEC* is favored because it produces a heat exchanger with good heat transfer and pressure loss performance. It is observed in Fig. 5(c) that the *PEC* for the perforated wavy fin with *r*=1.5mm is obviously higher than that of the others.

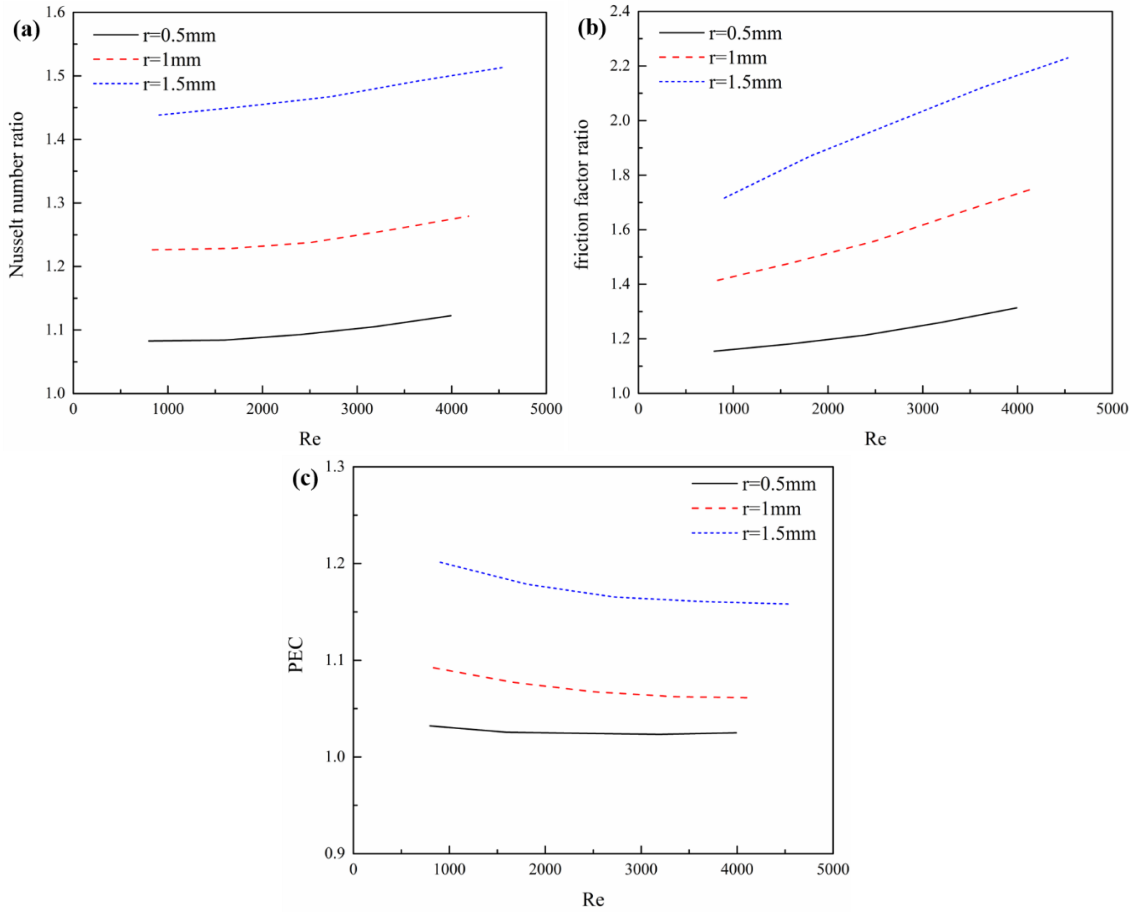

Figure 5. Influence of different perforated diameter on heat transfer performance with Reynolds number. (a) Nusselt number ratio; (b) friction factor ratio; (c) the PEC.

Preprints (www.preprints.org) | NOT PEER-REVIEWED | Posted: 24 April 2018 doi:10.20944/preprints201804.0304.v1

Peer-reviewed version available at Energies 2018, 11, 1398; doi:10.3390/en11061398

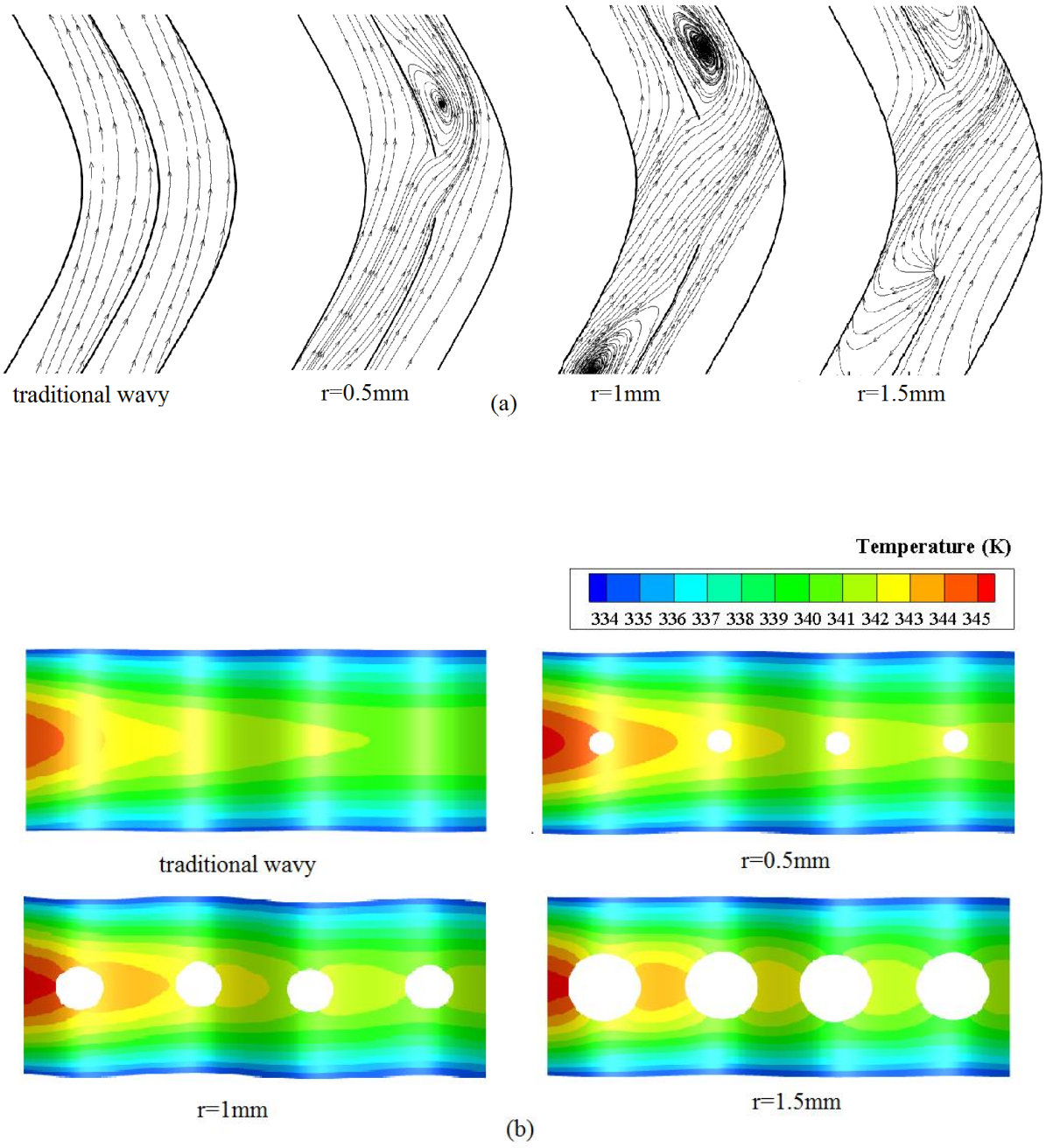

Figure 6. (a) Change in the streamline and **(b)** fin surface temperature distributions of the traditional wavy fin and perforated wavy fin when the radii are 0.5mm, 1mm and 1.5mm.

3.2. Influence of Different Stagger Ratio

Fig.7 shows, respectively the relations between the Nusselt number ratio ($Nu/Nu_{basic,wavy}$), friction factor ratio ($f/f_{basic,wavy}$) and the PEC under different stagger ratio. Fig.8 displays the change in the streamline, the fin surface temperature distribution of the traditional wavy fin and staggered wavy fin with different stagger ratio. The stagger ratios are 0.2, 0.3, and 0.4, respectively. In Fig. 7 (a), it is shown that the staggered wavy fin with stagger ratio $\beta = 0.4$ has

higher values of the Nusselt number ratio, which is all greater than 1 in the simulation range. It is observed in Fig.7 (b) that friction factor ratio of staggered wavy fin increases with the increase of the Reynolds number. It is important to note that within the simulation range, the friction factor ratio is observed to be less than 1 when Re is less than 2500, which is to say, the staggered structure is good for reducing the pressure drop. From the streamline shown in Fig.8 (a) it can be seen that, the greater stagger ratio, the less flow turbulence at the stagger section. At the same time, the increase of stagger ratio decreases the swirl flow near the fin surface which is beneficial for adequate heat transfer, as shown in Fig.8 (b), the larger the stagger ratio, the higher the surface temperature of the fin. Fig.7 (c) shows that the heat exchanger performance evaluation criteria for the staggered wavy fin with stagger ratio 0.4 is obvious compared to the others within the simulation range.

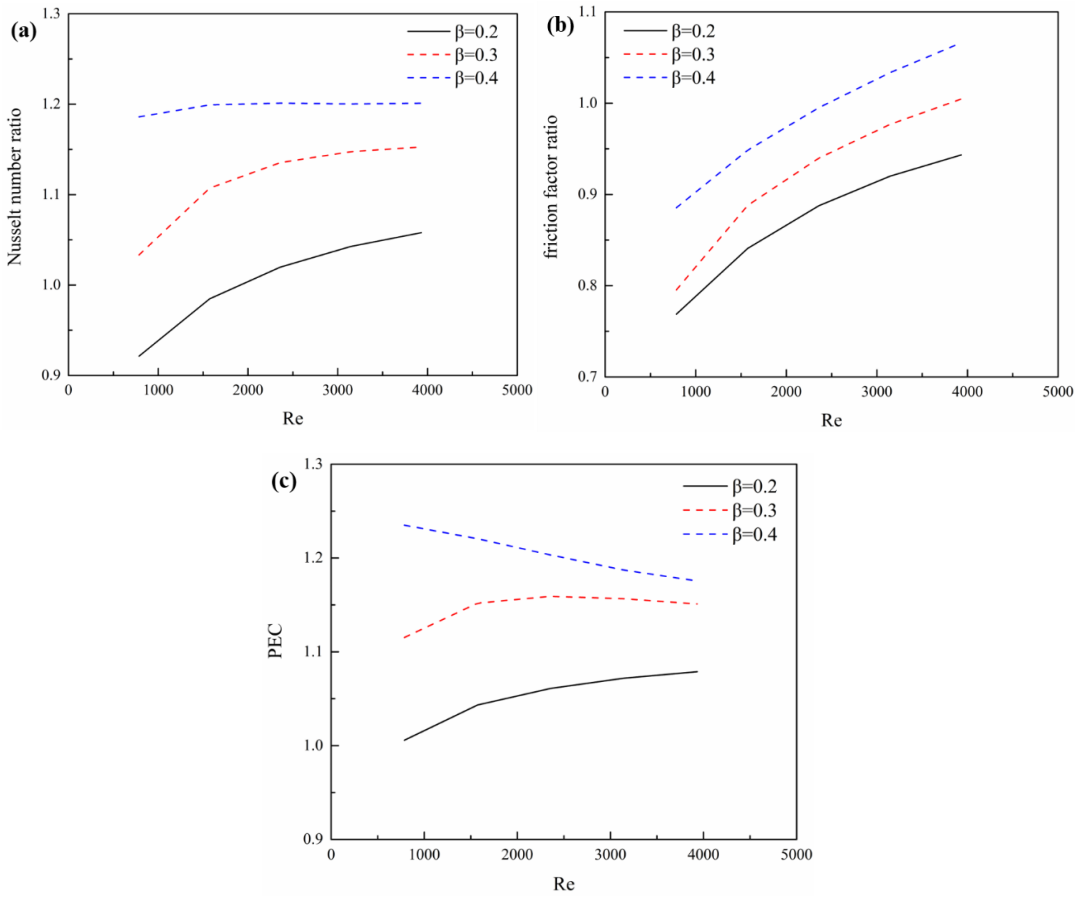

Figure 7. Influence of different stagger ratio on heat transfer performance with Reynolds number. **(a)** Nusselt number ratio; **(b)** friction factor ratio; **(c)** the PEC.

Preprints (www.preprints.org) | NOT PEER-REVIEWED | Posted: 24 April 2018 doi:10.20944/preprints201804.0304.v1

Peer-reviewed version available at Energies 2018, 11, 1398; doi:10.3390/en11061398

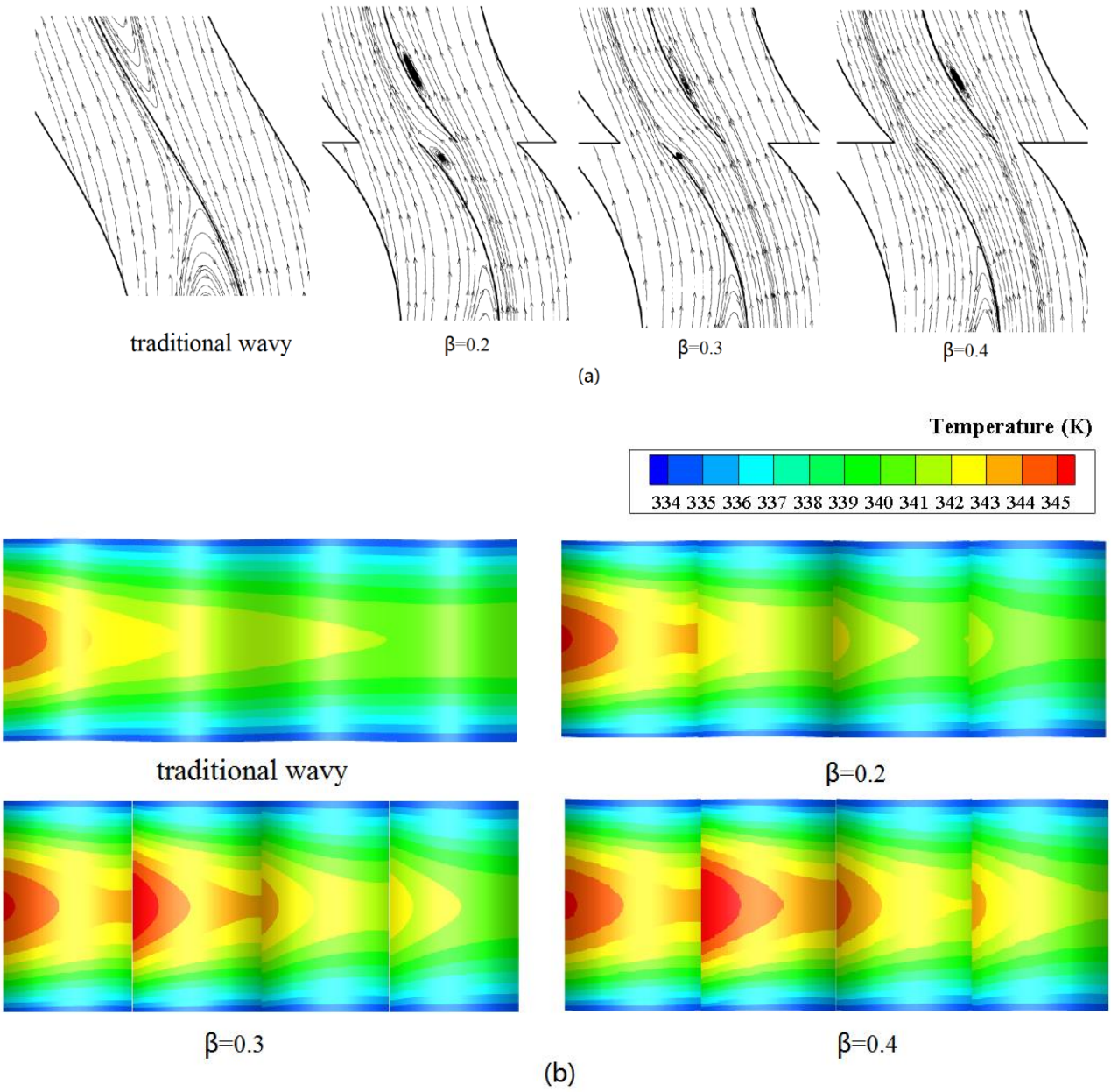

Figure 8. (a) Change in the streamline and **(b)** fin surface temperature distribution of the traditional wavy fin and staggered wavy fin when the stagger ratios are 0.2, 0.3 and 0.4.

3.3. Influence of Different Breaking Distance for Discontinuous Wavy Fin

Preprints (www.preprints.org) | NOT PEER-REVIEWED | Posted: 24 April 2018 doi:10.20944/preprints201804.0304.v1

Peer-reviewed version available at Energies 2018, 11, 1398; doi:10.3390/en11061398

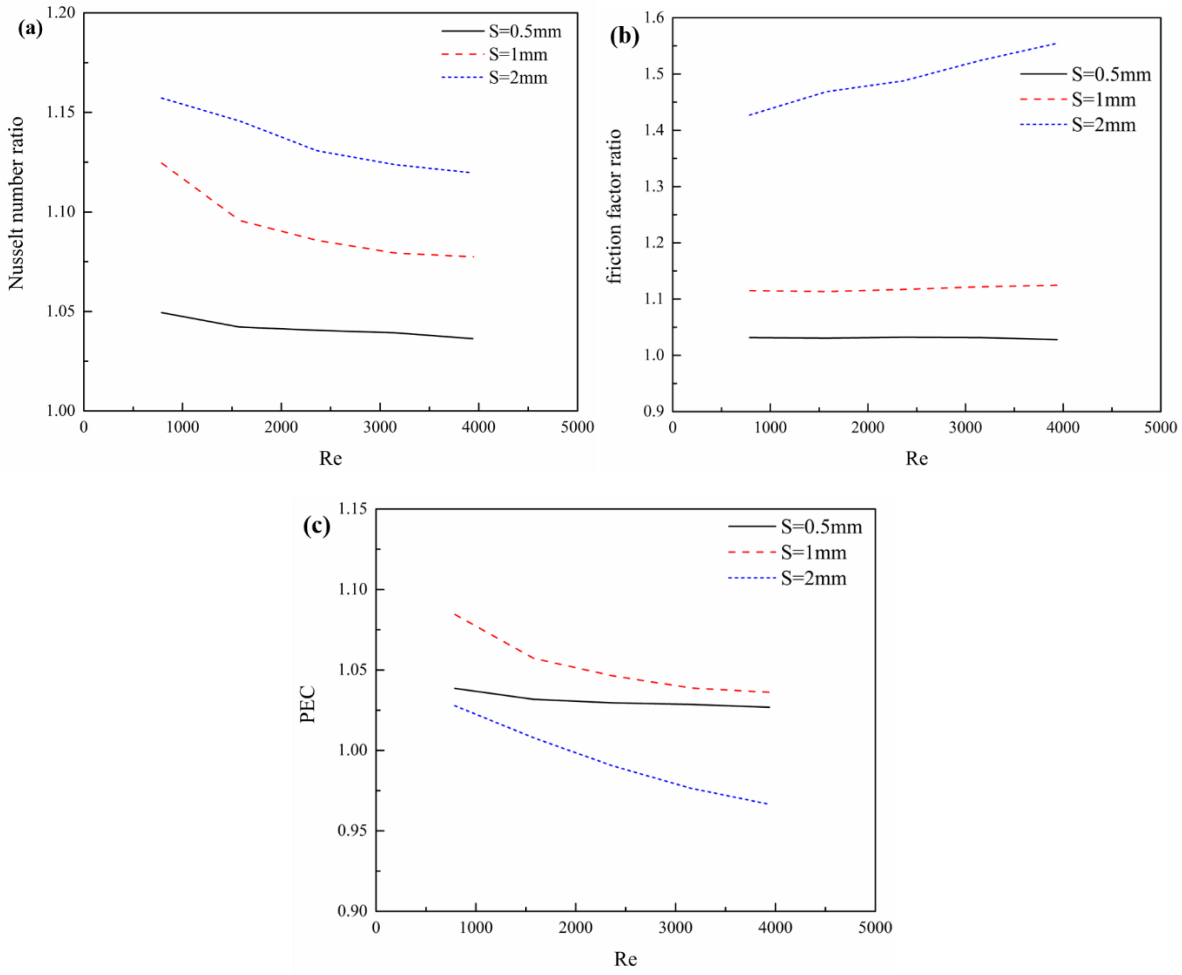

Figure 9. Influence of different breaking distance on heat transfer performance with Reynolds number. **(a)** Nusselt number ratio; **(b)** friction factor ratio; **(c)** the PEC.

Fig. 9 shows the relations between the Nusselt number ratio ($Nu/Nu_{basic,wavy}$), friction factor ratio ($f/f_{basic,wavy}$) and the *PEC* under different breaking distance, respectively. The change in the streamline and fin surface temperature distribution of the traditional wavy fin and discontinuous wavy fin with different breaking distance is showed in Fig.10. The distances are 0.5mm, 1mm, and 2mm, respectively. It is observed that the discontinuous wavy fin with large spacing has higher values of Nusselt number and friction factor. The friction factor ratio of discontinuous wavy fin increases with the increase of Re, the slope is maximum when the breaking distance is 2mm. The streamline shown in Fig. 10 (a) suggested that, the larger the distance between the discontinuous wavy fins, the better the mixing of fluid on both sides of the fin, thereby enhancing the heat transfer performance. At the same time, the increase of breaking distance increases the swirl flow near the fin surface. Fig. 10 (b) indicates that the temperature increases at the breaking edge of the second row, which mainly because that the discontinuous structure interrupts the development of both fluid boundary layer and thermal fluid boundary. Fig.9 (c) shows that the heat exchanger performance evaluation criteria for the discontinuous wavy fin with 1 mm spacing is highest.

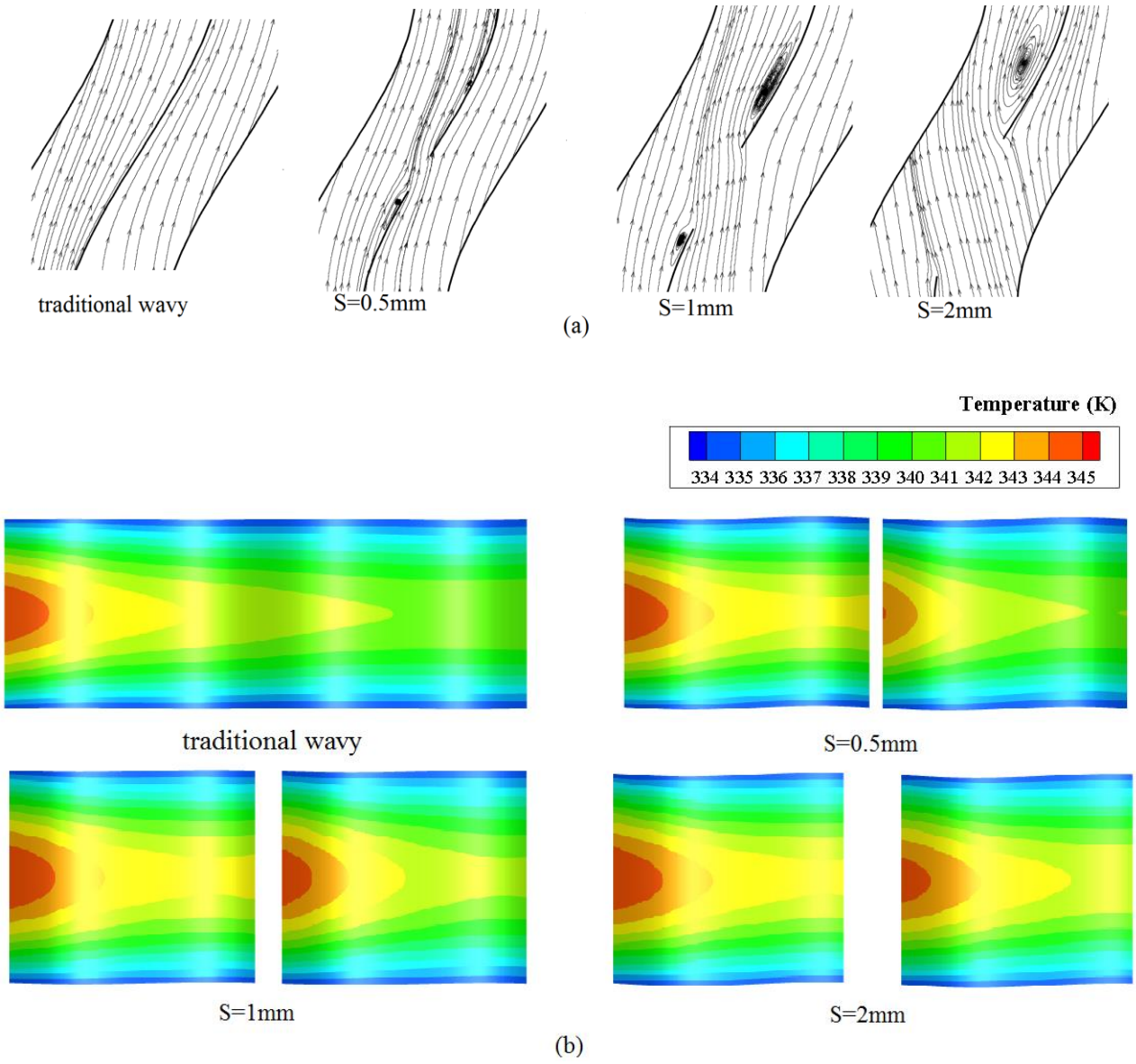

Figure 10. (a) Change in the streamline and **(b)** fin surface temperature distribution of the traditional wavy fin and discontinuous wavy fin when the breaking distances are 0.5mm, 1mm and 2mm.

3.4. Influence of Waviness Aspect Ratio of Different Wavy Fin

According to the results of previous studies, the perforated wavy fin with R=1.5 mm, staggered wavy fin with β=0.4 and discontinuous wavy fin with S=1 mm are chosen to compare with the traditional wavy fin at different waviness aspect ratio. In order to investigate the impacts of the waviness aspect ratio, three values are considered for this parameter (γ=0.38, 0.42 and 0.45).

The variations of the Nusselt number ratio ($Nu/Nu_{basic,wavy}$) over the three new kinds of wavy fins are shown in Fig.11 (a) to (c) for different waviness aspect ratio. As it can be seen, all curves have values higher than 1 which indicates that the applied techniques are beneficial for the heat transfer. It is found that the Nusselt number ratio of perforated wavy fin with r=1.5 mm increases with the increasing inlet velocity, and that of the discontinuous wavy fin remains almost constant slightly bigger than 1, while the Nusselt number ratio of staggered wavy fin decreases by increasing inlet velocity.

Preprints (www.preprints.org) | NOT PEER-REVIEWED | Posted: 24 April 2018 doi:10.20944/preprints201804.0304.v1

Peer-reviewed version available at Energies 2018, 11, 1398; doi:10.3390/en11061398

Obviously, it can be also observed that the Nusselt number ratio of the perforated wavy fin with r=1.5 mm is the highest in all cases. At the same time, with the increase of the waviness aspect ratio, the advantage of the perforated wavy fin is more obvious while that of the other two kinds of fins are slightly declining.

It indicates that the perforation and serration techniques are beneficial for the enhancement of heat transfer at different waviness aspect ratio, it is because the perforation and serration lead to collision among streamlines and thus the enhanced flow turbulence result in greater fluid mixing. Although the heat transfer performance of the discontinuous wavy fin is not much increased, the heat transfer area is reduced which is good for saving materials.

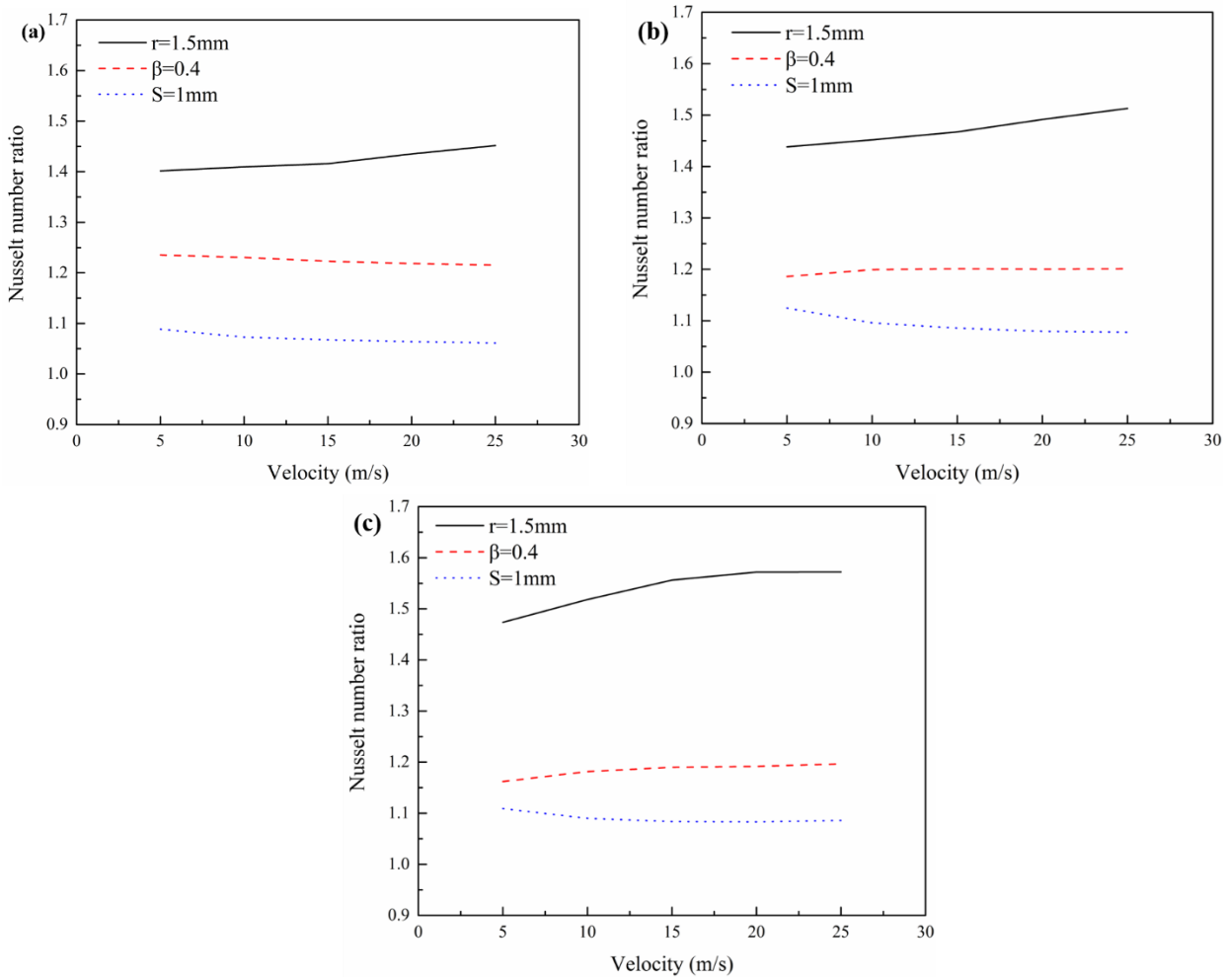

Figure 11. Nusselt number ratio versus the inlet velocity for three kinds of wavy fin with **(a)** γ=0.38, **(b)** γ=0.42, **(c)** γ=0.45.

The variations of friction factor ratio ($f/f_{basic,wavy}$) for the three kinds of wavy fins against the inlet velocity are shown in Fig.12 (a-c) for different waviness aspect ratio. At a given velocity, the friction factor ratio of perforated wavy fin with r=1.5 mm is the highest. This can be explained by strong flow fluctuation in the presence of holes on the fin surface. As it can be seen, with the increase of the waviness aspect ratio, the friction factor ratio decreases, especially for the discontinuous wavy fin, the friction factor ratio gradually becomes less than 1. The point is that the bigger waviness aspect ratio causes stronger swirl flow near the fin surface, and this trend is stronger in the traditional wavy fin than in the staggered wavy fin and discontinuous wavy fin as shown in Fig. 14.

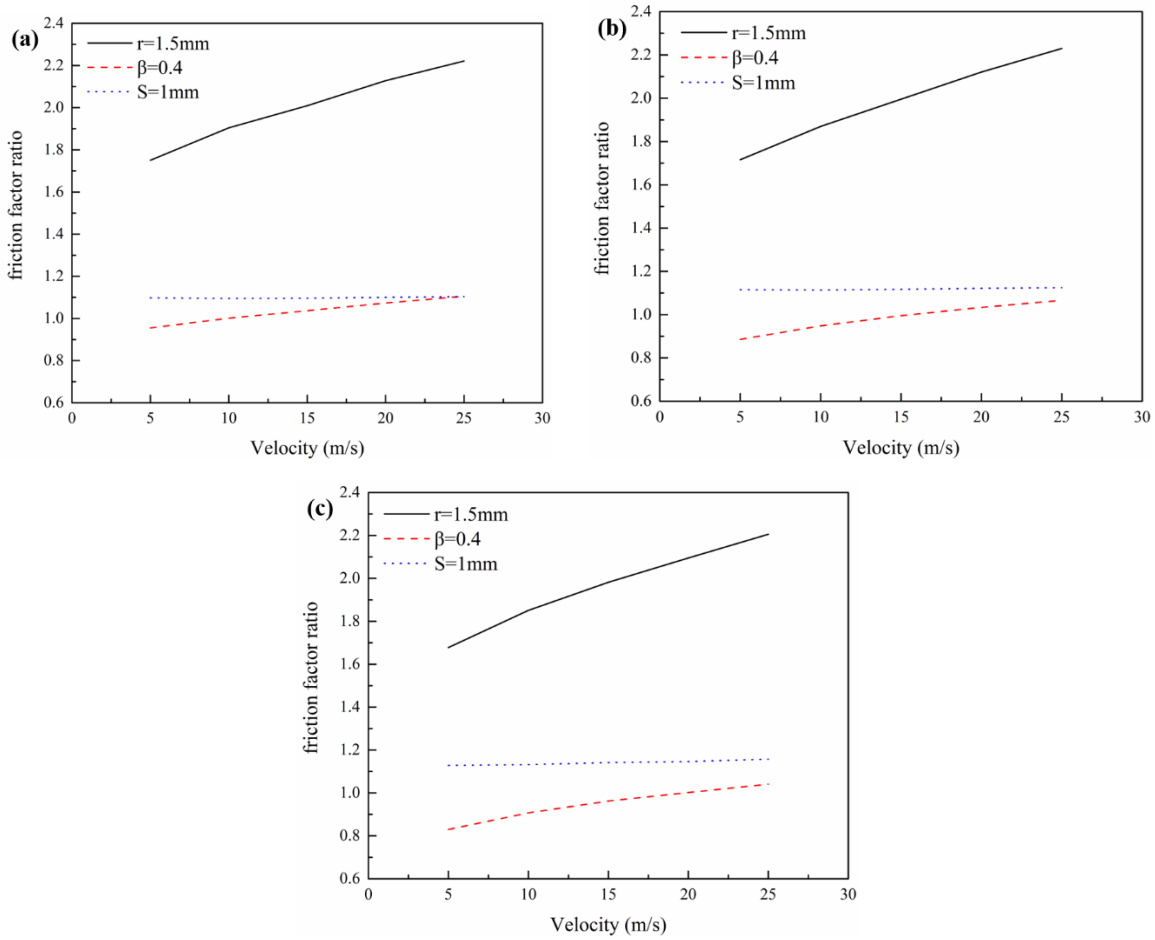

Figure 12. Friction factor ratio versus the inlet velocity for three kinds of wavy fin with **(a)** γ=0.38, **(b)** γ=0.42, **(c)** γ=0.45.

Preprints (www.preprints.org) | NOT PEER-REVIEWED | Posted: 24 April 2018 doi:10.20944/preprints201804.0304.v1

Peer-reviewed version available at Energies 2018, 11, 1398; doi:10.3390/en11061398

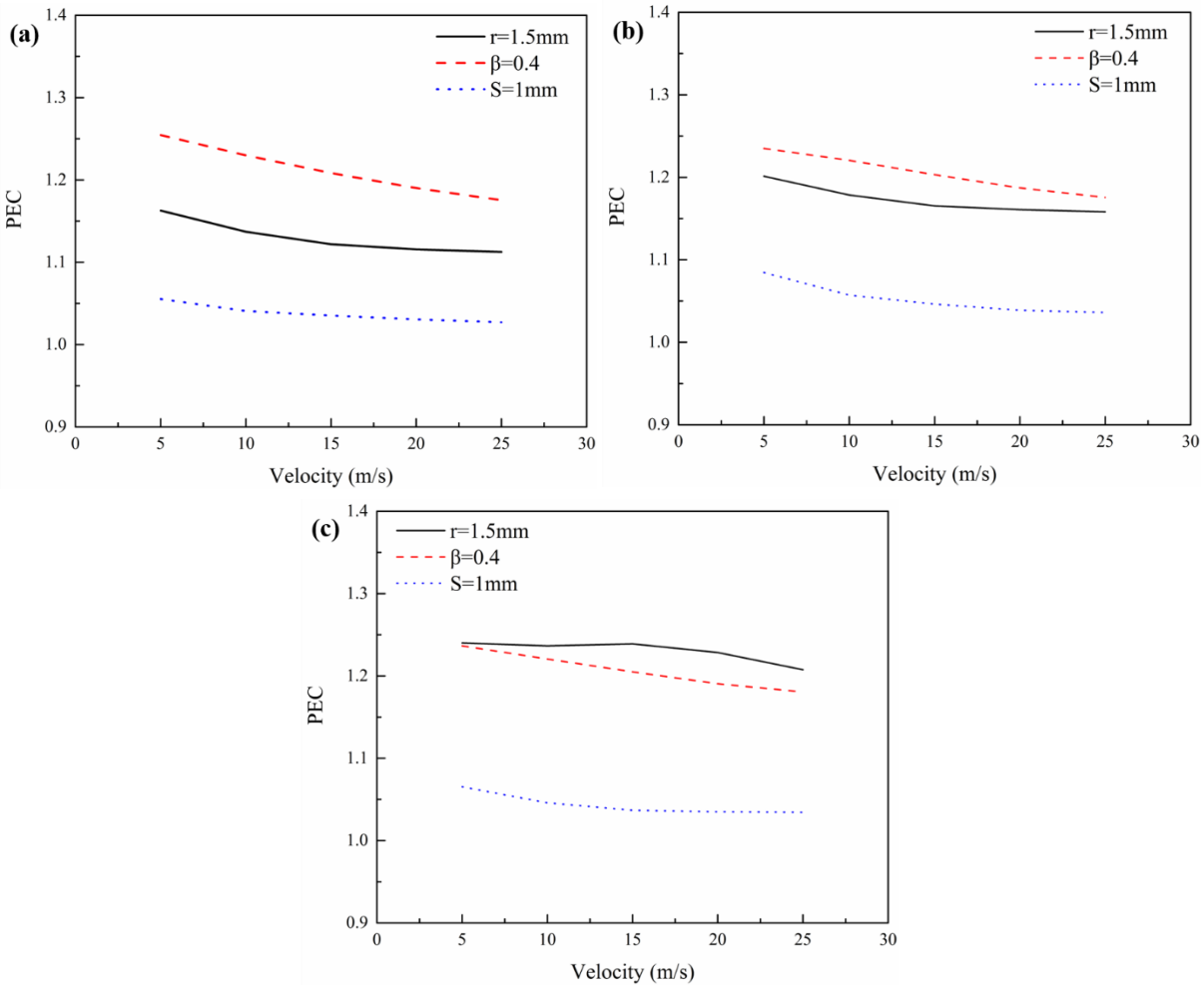

Figure 13. Thermal-hydraulic performance factor versus the inlet velocity for three kinds of wavy fin with **(a)** γ=0.38, **(b)** γ=0.42, **(c)** γ=0.45.

Fig. 13 (a-c) shows the variations of thermal-hydraulic performance factor over the three kinds of wavy fins for different waviness aspect ratio. The thermal-hydraulic performance factor of proposed wavy fins are all larger than 1. The change of thermal-hydraulic performance factor of the discontinuous wavy fin for different inlet velocity is small at different waviness aspect ratios. It is worth noting that with the increase of the waviness aspect ratio, the predominance of the staggered wavy fin is gradually surpassed by the perforated wavy fin. It means that using the serration technique in the smaller aspect ratio shows a considerable improvement in the thermal-hydraulic performance of the wavy fin. The maximum *PEC* of 1.24 is obtained for the perforated wavy fin at the largest waviness aspect ratio.

Preprints (www.preprints.org) | NOT PEER-REVIEWED | Posted: 24 April 2018 doi:10.20944/preprints201804.0304.v1

Peer-reviewed version available at Energies 2018, 11, 1398; doi:10.3390/en11061398

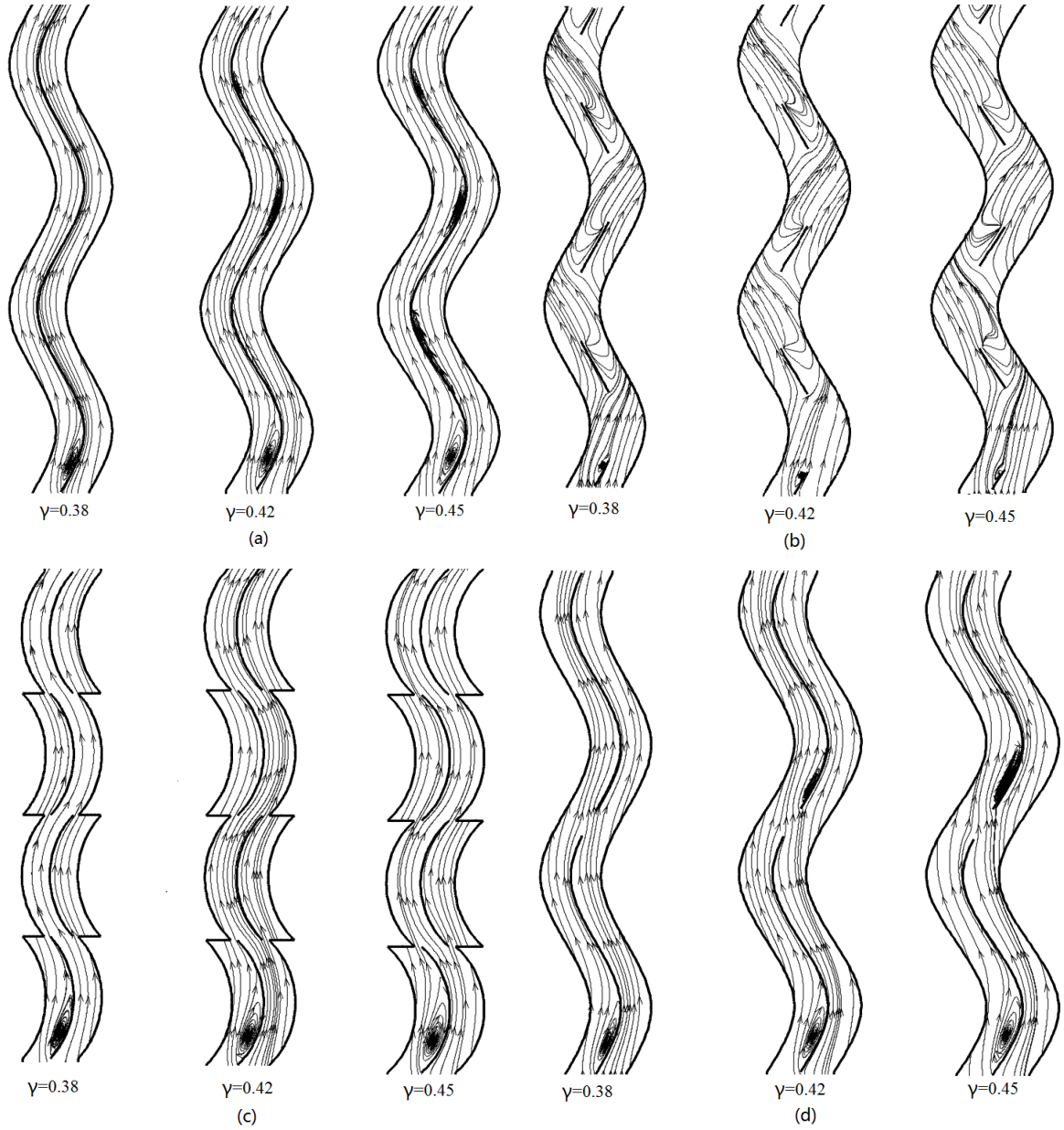

Figure 14. Change in the streamline of the **(a)** traditional wavy fin, **(b)** perforated wavy hole, **(c)** staggered wavy fin, and **(d)** discontinuous wavy fin when the waviness aspect ratio are 0.38, 0.42, and 0.45.

4. Conclusions

Three new kinds of wavy plate fins, namely perforated wavy fin, staggered wavy fin and discontinuous wavy fin are proposed and investigated by numerical simulation. The current study shows that the proposed perforation, serration and breaking technology may have advantages over the traditional wavy fins. The following results obtained can be beneficial to the improvement of air-side heat transfer performance of the plate fin heat exchanger.

(1) For perforated wavy fin, the enlarged hole can strengthen the flow turbulence, leading to a rapid mixing between the core and the fluid near the fin surface thus the bigger the holes, the better the thermal-hydraulic performance. For staggered wavy fin, the greater stagger ratio, the less flow turbulence at the stagger section and the larger the stagger ratio, the better the thermal-hydraulic performance. For discontinuous wavy fin, the larger the distance between the discontinuous wavy fins, the better the mixing of fluid on both sides of the fin thereby enhancing the heat transfer performance. At the same time, the friction factor has increased dramatically when the breaking distance is 2 mm.

Peer-reviewed version available at Energies 2018, 11, 1398; doi:10.3390/en11061398

(2) The Nusselt number and friction factor of the perforated wavy fin are all higher than that of the traditional wavy fin. The serration technology is beneficial to reduce the friction factor compared to the traditional wavy fin. Using the serration technique in the smaller aspect ratio shows a considerable improvement in the thermal-hydraulic performance of the wavy fin.

(3) At a given inlet velocity, Nusselt number and the *PEC* for the three proposed new wavy fins are higher than that for the traditional wavy fin, and it tends to almost invariable with increasing waviness aspect ratio for discontinuous wavy fin. At the same time, with increasing of waviness aspect ratio, the *PEC* for the perforated wavy fin and staggered wavy fin increases. And the predominance of the staggered wavy fin is gradually surpassed by the perforated wavy fin.

(4) The present study shows that the proposed heat transfer enhancement techniques are all have advantages over the traditional wavy fin. Perforation is beneficial to enhance the heat transfer, improve the Nusselt number, serration is beneficial to reduce the friction factor, and the breaking technique can reduce heat transfer area while enhancing heat transfer performance.

Nomenclature

A	Total heat transfer area, m^2
A_c	Minimum free flow area, m^2
a	wave amplitude, mm
C_p	specific heat at constant pressure, kJ/(kg·K)
D_h	hydraulic diameter, mm
F_c	Stagger spacing, mm
F_h	Fin height, mm
F_p	Fin pitch, mm
f	friction factor
G	mass velocity, kg/(m^2·s)
h	heat transfer coefficient, W/(m^2·K)
j	Colburn factor
L	Flow length, mm
L_z	Wavy fin passage length, mm
l	wavy length, mm
m	Mass flow rate, kg/s
Nu	Nusselt number
Pr	Prandtl number
p	pressure, Pa
PEC	Performance evaluation criteria
Q	Heat flow, W
r	Perforation radius, mm
Re	Reynolds number
S	Spacing in discontinuous wavy fin, mm; mean rate of strain tensor.
T	temperature, K
V	Air inlet velocity, m/s

u_i	Velocity in the i direction, m/s
u_j	Velocity in the j direction, m/s
x_i	Coordinate, m

Greek letters

ρ	Fluid density, kg/m^3
μ	dynamic viscosity, Pa·s
γ	waviness aspect ratio
δ	Fin thickness, mm
β	Stagger ratio
τ	Shear stress, Pa
λ	Thermal conductivity, W/(m·K)
η	Fin efficiency

Subscripts

f	fin
in	inlet
out	outlet
p	plate
w	wall

Acknowledgments: The financial supports for this research project from the National Natural Science Foundation of China (No. 51676069), the national "973 Program" of China (No. 2015CB251503) and the Fundamental Research Funds for the Central Universities of Ministry of Education of China (No. 2016XS134) are gratefully acknowledged.

References

1. F.V. Tinaut, A. Melgar, A.A.R. Ali, Correlations for heat transfer and flow friction characteristics of compact plate-type heat exchangers, International Journal of Heat & Mass Transfer, 35(7) (1992) 1659-1665.
2. L.S. Ismail, R. Velraj, C. Ranganayakulu, Studies on pumping power in terms of pressure drop and heat transfer characteristics of compact plate-fin heat exchangers—A review, Renewable & Sustainable Energy Reviews, 14(1) (2010) 478–485.
3. M. Yousefi, R. Enayatifar, A.N. Darus, Optimal design of plate-fin heat exchangers by a hybrid evolutionary algorithm ☆, International Communications in Heat & Mass Transfer, 38(10) (2011) 258-263.
4. C. T'Joen, A. Jacobi, M.D. Paepe, Flow visualisation in inclined louvered fins, Experimental Thermal & Fluid Science, 33(4) (2009) 664-674.
5. A. Vaisi, M. Esmaeilpour, H. Taherian, Experimental investigation of geometry effects on the performance of a compact louvered heat exchanger, Applied Thermal Engineering, 31(16) (2011) 3337-3346.
6. W.M. Kays, A.L. London, Compact heat exchangers, Journal of Applied Mechanics, 27(2) (1984) 460-470.
7. M. Khoshvaght-Aliabadi, F. Hormozi, A. Zamzamian, Role of channel shape on performance of plate-fin heat exchangers: Experimental assessment, International Journal of Thermal Sciences, 79 (2014) 183-193.
8. J. Du, Z.Q. Qian, Z.Y. Dai, Experimental study and numerical simulation of flow and heat transfer performance on an offset plate-fin heat exchanger, Heat and Mass Transfer, 52(9) (2016) 1-16.
9. J. Dong, J. Chen, W. Zhang, J. Hu, Experimental and numerical investigation of thermal-hydraulic performance in wavy fin-and-flat tube heat exchangers, Applied Thermal Engineering, 30(11–12) (2010) 1377-1386.

10. A. Joardar, A.M. Jacobi, Impact of leading edge delta-wing vortex generators on the thermal performance of a flat tube, louvered-fin compact heat exchanger, International Journal of Heat and Mass Transfer, 48(8) (2005) 1480-1493.
11. B. Lotfi, B. Sundén, Q. Wang, An investigation of the thermo-hydraulic performance of the smooth wavy fin-and-elliptical tube heat exchangers utilizing new type vortex generators, Applied Energy, 162 (2016) 1282-1302.
12. L.H. Tang, W.X. Chu, N. Ahmed, M. Zeng, A new configuration of winglet longitudinal vortex generator to enhance heat transfer in a rectangular channel, Applied Thermal Engineering, 104 (2016) 74-84.
13. H. Peng, L. Xiang, J. Li, Performance investigation of an innovative offset strip fin arrays in compact heat exchangers, Energy Conversion & Management, 80(80) (2014) 287-297.
14. A.H. Alessa, A.M. Maqableh, S. Ammourah, Enhancement of natural convection heat transfer from a fin by rectangular perforations with aspect ratio of two, International Journal of Physical Sciences, 4(10) (2009) 540-547.
15. M.R. Shaeri, M. Yaghoubi, K. Jafarpur, Heat transfer analysis of lateral perforated fin heat sinks, Applied Energy, 86(10) (2009) 2019-2029.
16. E.H. Ridouane, A. Campo, Heat Transfer Enhancement of Air Flowing Across Grooved Channels: Joint Effects of Channel Height and Groove Depth, Journal of Heat Transfer, 130(2) (2008) 281-293.
17. L. Tian, B. Liu, C. Min, J. Wang, Y. He, Study on the effect of punched holes on flow structure and heat transfer of the plain fin with multi-row delta winglets, Heat and Mass Transfer, 51(11) (2015) 1523-1536.
18. X. Du, L. Feng, Y. Yang, L. Yang, Experimental study on heat transfer enhancement of wavy finned flat tube with longitudinal vortex generators, Applied Thermal Engineering, 50(1) (2013) 55-62.
19. G. Lu, G. Zhou, Numerical simulation on performances of plane and curved winglet type vortex generator pairs with punched holes, International Journal of Heat and Mass Transfer, 102 (2016) 679-690.
20. C.H. Jeong, H.R. Kim, M.Y. Ha, S.W. Son, J.S. Lee, P.Y. Kim, Numerical investigation of thermal enhancement of plate fin type heat exchanger with creases and holes in construction machinery, Applied Thermal Engineering, 62(2) (2014) 529-544.
21. H.S. Ahn, S.W. Lee, S.C. Lau, Heat Transfer Enhancement for Turbulent Flow Through Blockages With Round and Elongated Holes in a Rectangular Channel, Journal of Heat Transfer, 129(11) (2007) 1611-1615.
22. W.M. Kays, A.L. London, Compact Heat Exchangers /-Third Edition, McGraw-Hill Book Company, 1984.
23. D. Junqi, C. Jiangping, C. Zhijiu, Z. Yimin, Z. Wenfeng, Heat transfer and pressure drop correlations for the wavy fin and flat tube heat exchangers, Applied Thermal Engineering, 27(11-12) (2007) 2066-2073.

Figure captions

Figure 1. The shape of (a) traditional wavy fin; (b) perforated wavy fin; (c) staggered wavy fin type; (d) discontinuous wavy fin.

Figure 2. Computational domains and boundary details for the staggered wavy fin.

Figure 3. Change in the *j*-factor in accordance with the change of grids munber.

Figure 4. Comparison between the values of the (a) *j*-factor and (b) *f*-factor using different turbulent flow models.

Figure 5. Influence of different perforated diameter on heat transfer performance with Reynolds number. (a) Nusselt number ratio; (b) friction factor ratio; (c) the *PEC*.

Figure 6. (a) Change in the streamline and (b) fin surface temperature distributions of the traditional wavy fin and perforated-wavy fin when the radii are 0.5mm, 1mm and 1.5mm.

Figure 7. Influence of different stagger ratio on heat transfer performance with Reynolds number. (a) Nusselt number ratio; (b) friction factor ratio; (c) the *PEC*.

Figure 8. (a) Change in the streamline and (b) fin surface temperature distribution of the traditional wavy fin and staggered-wavy fin when the stagger ratios are 0.2, 0.3 and 0.4.

Figure 9. Influence of different breaking distance on heat transfer performance with Reynolds number. (a) Nusselt number ratio; (b) friction factor ratio; (c) the PEC.

Figure 10. (a) Change in the streamline and (b) fin surface temperature distribution of the traditional wavy fin and discontinuous wavy fin when the breaking distances are 0.5mm, 1mm and 2mm.

Figure 11. Nusselt number ratio versus the inlet velocity for three kinds of wavy fin with (a) γ=0.38, (b) γ=0.42, (c) γ=0.45.

Figure 12. Friction factor ratio versus the inlet velocity for three kinds of wavy fin with (a) γ=0.38, (b) γ=0.42, (c) γ=0.45.

Figure 13. Thermal-hydraulic performance factor versus the inlet velocity for three kinds of wavy fin with (a) γ=0.38, (b) γ=0.42, (c) γ=0.45.

Figure 14. Change in the streamline of the (a) traditional wavy fin, (b) perforated wavy hole, (c) staggered wavy fin, and (d) discontinuous wavy fin when the waviness aspect ratio are 0.38, 0.42, and 0.45.